ICES Journal of
Marine Science

ICES Journal of Marine Science (2016), 73(7), 1725–1738. doi:10.1093/icesjms/fsw036

Editor's Choice

Integrating spatial synchrony/asynchrony of population distribution into stock assessment models: a spatial hierarchical Bayesian statistical catch-at-age approach

Yan Jiao[1]*, Rob O'Reilly[2], Eric Smith[3], and Don Orth[1]

[1]*Department of Fish and Wildlife Conservation, Virginia Polytechnic Institute and State University, 100 Cheatham Hall, Blacksburg, VA 24061-0321, USA*
[2]*Virginia Marine Resources Commission, 2600 Washington Avenue, Newport News, VA 23607, USA*
[3]*Department of Statistics, Virginia Polytechnic Institute and State University, Blacksburg, VA 24061-0321, USA*

**Corresponding author: tel: +1 540 231 5749; fax: +1 540 231 7580; e-mail: yjiao@vt.edu*

Jiao, Y., O'Reilly, R., Smith, E., and Orth, D. Integrating spatial synchrony/asynchrony of population distribution into stock assessment models: a spatial hierarchical Bayesian statistical catch-at-age approach. – ICES Journal of Marine Science, 73: 1725–1738.

Received 20 May 2015; revised 7 February 2016; accepted 21 February 2016.

In many marine fisheries assessments, population abundance indices from surveys collected by different states and agencies do not always agree with each other. This phenomenon is often due to the spatial synchrony/asynchrony. Those indices that are asynchronous may result in discrepancies in the assessment of temporal trends. In addition, commonly employed stock assessment models, such as the statistical catch-at-age (SCA) models, do not account for spatial synchrony/asynchrony associated with spatial autocorrelation, dispersal, and environmental noise. This limits the value of statistical inference on key parameters associated with population dynamics and management reference points. To address this problem, a set of geospatial analyses of relative abundance indices is proposed to model the indices from different surveys using spatial hierarchical Bayesian models. This approach allows better integration of different surveys with spatial synchrony and asynchrony. We used Atlantic weakfish (*Cynoscion regalis*) as an example for which there are state-wide surveys and expansive coastal surveys. We further compared the performance of the proposed spatially structured hierarchical Bayesian SCA models with a commonly used Bayesian SCA model that assumes relative abundance indices are spatially independent. Three spatial models developed to mimic different potential spatial patterns were compared. The random effect spatially structured hierarchical Bayesian model was found to be better than the commonly used SCA model and the other two spatial models. A simulation study was conducted to evaluate the uncertainty resulting from model selection and the robustness of the recommended model. The spatially structured hierarchical Bayesian model was shown to be able to integrate different survey indices with/without spatial synchrony. It is suggested as a useful tool when there are surveys with different spatial characteristics that need to be combined in a fisheries stock assessment.

Keywords: Atlantic weakfish, spatial hierarchical Bayesian model, spatial synchrony/asynchrony, statistical catch-at-age.

Introduction

Many marine fisheries assessments require the modeller to combine survey population abundance indices from different states and agencies. A potentially important problem is that the indices do not always agree with each other and the use of different indices may lead to different decisions (NEFSC, 2008; NDPSWG, 2009). The discrepancy among different survey indices can be attributed to the spatial and temporal aggregation of fish distributions, non-random search behaviour of fishers, fishing power changes, gear selectivity, gear saturation, and other factors (Pope and Garrod, 1975; MacCall, 1976; Rose and Leggett, 1991). Spatial heterogeneity refers to the uneven distribution of observations of interest, such as a trait, event, fish abundance, density, or relationship across a region (Anselin, 2010). Even for well-designed surveys, the indices of abundance can suggest different trends at different locations because of temporal changes in the densities of the population in different locations, shown as spatial asynchronous patterns (Buonaccorsi *et al.*, 2001; Liebhold *et al.*, 2004). Spatial heterogeneity among locations may not change over time but if it does change it would show as spatial asynchrony. Reasons for spatial synchrony/asynchrony include extrinsic environmental stochasticity (Moran effect; Moran, 1953), non-linear density-dependency, and dispersal and species interactions (Heino *et al.,* 1997; Hudson and Cattadori, 1999; Buonaccorsi *et al.,* 2001; Cheal *et al.,* 2007; Vasseur, 2007; Haynes *et al.,* 2009; Massie *et al.,* 2015).

Atlantic weakfish (*Cynoscion regalis*) is used as an example stock in our study. It is very representative of the species along the western coast of the Atlantic Ocean because the surveys available for Atlantic weakfish are also available for most other species distributed in this area. Each state along the North Atlantic has its own localized surveys, and there are also two expansive coastal surveys for this species (Supplementary Table S1; Figure 1). The discrepancy among different survey indices is considerable (NEFSC, 2009). A preliminary analysis based on cross correlation among relative abundance indices that are not standardized, but were reported by each state and agency (NEFSC, 2009), indicated that most of the

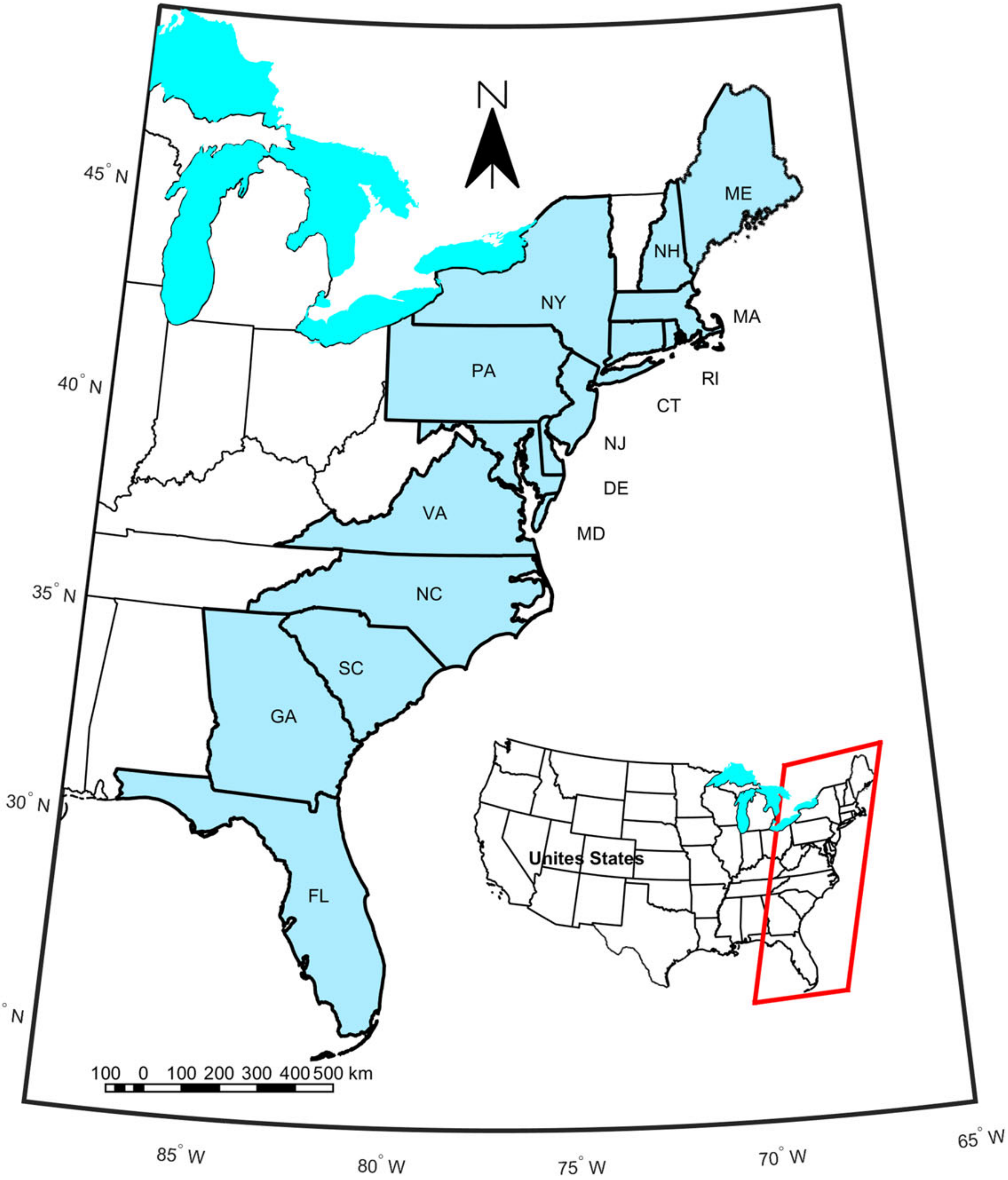

Figure 1. Map of western Atlantic with states that handle Atlantic weakfish surveys indicated. This figure is available in black and white in print and in colour at *ICES Journal of Marine Science* online.

correlations were low and many show no relationship or even have negative relationships (Supplementary Table S2a).

Standardization of the catch rate from the surveys or from the fisheries has been found to potentially eliminate the influence of a variety of factors such as the spatial and temporal aggregation of fish distribution, nonrandom search behaviour of fishers, gear saturation, water temperature, and other possible environmental factors that may influence the distribution and density of the fish (O'Brien and Mayo, 1988; Lo *et al.*, 1992; Maunder and Punt, 2004; Yu *et al.*, 2011). However, standardization itself cannot guarantee that the true overall population size is well represented by each of the localized surveys because of strong changes in fish distributions, habitat types, non-linear response to local population density and dispersal, etc. These similarities and discrepancies among population indices over time are described as spatial synchrony and asynchrony (Vasseur, 2007; Pandit and Kolasa, 2012). Our preliminary analysis based on the standardized relative abundance indices suggested that standardization of weakfish indices did not remove survey index discrepancy (Winter *et al.*, 2009; Supplementary Table S2b).

Spatial autocorrelation, the dependence among observations over geographic space, has been used to model observed spatial heterogeneity or spatial synchrony/asynchrony (Heino *et al.*, 1997; Schabenberger and Gotway, 2005; Vasseur, 2007). Spatial autocorrelation often exists among ecological variables and may cause significant errors in data analyses and population dynamics modelling if neglected (Legendre, 1993; Heino *et al.*, 1997; Lawson *et al.*, 2003; Vasseur, 2007). Commonly employed stock assessment models, such as statistical catch-at-age (SCA) models, do not account for spatial synchrony/asynchrony among these fishery-independent/dependent surveys when relative abundance indices are used to calibrate population size. This limits the statistical inference for resulting key parameters of population dynamics and management reference points.

Our objectives are to account for spatial synchrony/asynchrony caused by spatial autocorrelation, dispersal, and environmental noises and to evaluate the appropriateness of using spatial hierarchical models with SCA models. We modelled relative abundance indices from different surveys, as spatially autocorrelated, through spatial hierarchical Bayesian models. These models of relative abundance indices were then integrated with a statistical catch-at-age model to allow better integration of different surveys. To test the efficiency of the proposed spatial hierarchical Bayesian SCA models in modelling spatial synchrony/asynchrony among survey indices and the uncertainty from model selection, a simulation study was conducted based on the example weakfish stock (Schnute, 1987; Jiao *et al.*, 2009a, b; Toni and Stumpf, 2010). Bayesian estimators were used to estimate parameters, and performance of the models was compared by their goodness-of-fit and the retrospective error evaluation of the models (Calder *et al.*, 2003; Jiao *et al.*, 2009a, b, 2010, 2012). The hierarchical spatially structured Bayesian models developed here, and the framework for modelling population dynamics using age-structured models with different relative abundance indices are applicable to many other species when there are many surveys with different spatial structures and when their relative abundance indices suggest different population trends.

Data and methods

The Atlantic weakfish population was selected as an example and its most recent stock assessment information was used. Data used were from the Atlantic States Marine Fisheries Commission Weakfish Technical Committee (NEFSC, 2009). Detailed information on the catch-at-age matrix and relative abundance surveys are available from the same report. Following the recommendation from the weakfish technical committee, catch data from 1982 to 2007 were used (Supplementary Figure S1). There were 15 relative abundance indices available for this fishery (Supplementary Figure S2). Among them, six provided age-structured relative abundance indices (Supplementary Figure S2a), and eight of them provided age 1 relative abundance that were used in the assessment to calibrate recruitment dynamics (Supplementary Figure S2b and Table S1). Detailed description on the relative abundance indices is given in Supplementary data, Table S1.

A series of stochastic age-structured models was constructed to represent the dynamics of the weakfish stock with different assumptions about spatial heterogeneity over time. The models consist of three submodels including (i) an age-structured process model that describes the dynamics of the population, (ii) an observation model that describes the relationship between estimated catch and observed catch in the fishery, and (iii) a series of observation models that describe the relationship between stock abundance and abundance indices observed in the fishery or fisheries-independent surveys. For the observation models of relative abundance indices, model 1 (M1) is commonly used, which uses a proportional relationship between abundance indices and stock abundance with a lognormal error distribution; model 2 (M2) is based on a random effect model; model 3 (M3) uses a conditional autoregressive model with correlations among neighbouring surveys accounted for; and model 4 (M4) uses a spatially autocorrelated model with correlation modelled as a function of distance between surveys. The four models are described below.

A common statistical catch-at-age model

A commonly used statistical catch-at-age separable model (SCA M1) based on the data structure of weakfish can be written as follows:

$$
\begin{aligned}
&\mathrm{Ln}(N_{a+1,y+1}) = \mathrm{Ln}(N_{a,y}\mathrm{e}^{-F_{a,y}-M})\\
&\mathrm{Ln}(C_{a,y}) = \mathrm{Ln}\left[\frac{F_{a,y}}{F_{a,y}+M}N_{a,y}(1-\mathrm{e}^{-F_{a,y}-M})\right] + \varepsilon_C\\
&F_{a,y} = F_y S_a\\
&\mathrm{Ln}(I_{j,a,y}) = \mathrm{Ln}(q_{j,a}N_{a,y}) + \varepsilon_{j,1}\\
&N_{a=1,y} = R_y \quad \text{and} \quad \ln(R_y) = \ln(\bar{R}) + \varepsilon_R\\
&\ln(N_{a>1,y=1982}) = \ln(\bar{N}_{a>1,y=1982}) + \varepsilon_N\\
&M = \text{known constant},
\end{aligned}
\tag{1}
$$

where a is age, y is year, N is population abundance and $\mathrm{Ln}(N_{a,y})$ means log-transformed $N_{a,y}$, C is observed catch and $\mathrm{Ln}(C_{a,y})$ is assumed to follow a normal distribution with error ε_C, F is fishing mortality and M is natural mortality, R is recruitment and we assumed that $\mathrm{Ln}(R_y)$ followed a normal distribution with mean $\mathrm{Ln}(\bar{R})$ and error ε_R, S is the selectivity, which is treated as age-specific (S_a) and does not change over time, j is the jth type of fishery dependent or independent cpue data. $\mathrm{Ln}(N_{a>1,y=1982})$ is the population size of age a in year 1982, and we assume that it follows a normal distribution with mean $\mathrm{Ln}(\bar{N}_{a>1,y=1982})$ and error ε_N. The errors associated with $\mathrm{Ln}(C_{a,y})$, $\mathrm{Ln}(R_y)$, and $\mathrm{Ln}(N_{a>1,y=1982})$ are assumed to have normal distributions with mean 0 and variance σ_c^2, σ_R^2, and σ_N^2 separately. The error associated with abundance index j, $\varepsilon_{j,1}$, is assumed to have mean 0 and variance σ_j^2. Here because the indices were dealt with in different ways and their variance assumptions are different in different models, we used numbers to represent their variances from models 1 to 4. In this model, M is assumed to be known and fixed at 0.25 and is constant among age groups and years (ASMFC, 2006; NEFSC, 2009). We used a constant vector to model selectivity instead of a logistic curve because the catch-at-age matrix is composed of catches from different fisheries, including trawl, gillnet, poundnet, and recreational fisheries, so the selectivity can be less regular. The initial numbers of population-at-age are estimated, and a uniform prior is used, i.e. $\bar{N}_{a>1,y=1982} \sim U(1, 100) \times C_{a,y=1982}$ with the Bayesian estimation process. The exploitation rate in 1982 was assessed to be >1 from a previous stock assessment, so using the observed $C_{a,y=1982}$ as the lower bound of $\bar{N}_{a>1,y=1982}$, and using $100 \times C_{a,y=1982}$ as the upper bound of $\bar{N}_{a>1,y=1982}$ is biologically reasonable and not restrictive as a prior. The variable R_y has been found to be highly variable and spawning stock size often only explains a limited amount of recruitment variation. So, we assume recruitment in year y,R_y, as a parameter to estimate rather than model using a regulated curve such as the Cushing and Beverton–Holt model (Ricker, 1975; Quinn and Deriso, 1999). Recruitment is assumed to have a two-level hierarchically structured prior (Table 1). If we use $C_{\text{cohort},y}$ to represent the total catch over time from the cohort of year y, then for a vague informative prior, we used $\ln(\bar{R}_y) \sim U\{\min[\ln(C_{1,y=1982:2007})], \max[\ln(100C_{\text{cohort},y})]\}$, for the minimum observed catch of age 1 fish, 1982–2007, we used $\min[\ln(C_{1,y=1982:2007})]$, and for the maximum observed $100 \times C_{\text{cohort},y}$ from 1982 to 2007, we used $\max[\ln(100C_{\text{cohort},y})]$. Given the levels of fishing mortality and natural mortality for Atlantic weakfish, using minimum observed catch as the lower bound of the mean of recruitment, and $\max[\ln(100C_{\text{cohort},y})]$ as the upper bound of the mean of recruitment is biologically reasonable and not restrictive. Recruitment was assumed to follow a lognormal distribution (see Equation 1) and stock recruitment dynamics were analysed outside of the statistical catch-at-age models. This will also avoid the influence of recruitment modelling choices on the hierarchical models of the relative abundance indices. The prior for F_y is assumed to be uniform between 0.001 and 2, that of S_a is uniform between 0 and 1, that of $q_{j,a=1}$ to be between $\min(I_{j,a=1}/\text{upper bound of } \bar{R})$ and $\max(I_{j,a=\,1}/\text{lower bound of } \bar{R})$, and that of $q_{j,a>1}$ to be between $\min(I_{j,a>1,y}/100C_{a>1,y})$ and $\max(I_{j,a>1,y}/C_{a>1,y})$.

Hierarchical spatial Bayesian statistical catch-at-age models that fit the relative abundance indices as spatially autocorrelated (M2–M4)

The second model is similar to model M1 except that the populations being sampled by the various surveys, $N_{j,a,y}$, are assumed to be different for different survey locations, i.e. are treated as random effects, and were modelled hierarchically (SCA_RE, **M2**),

$$\begin{aligned} \text{Ln}(I_{j,a,y}) &= \text{Ln}(q_{j,a}N_{j,a,y}) + \varepsilon_{j,a,y,2} \\ N_{j,a,y} &\sim \text{Log-}N(\text{Ln}(N_{a,y}), \sigma^2_{y,a,N,2}), \end{aligned} \tag{2}$$

where Log-N means lognormal distribution; variance $\sigma^2_{y,a,N}$ is the variance of log-transformed $N_{a,y}$; $\varepsilon_{j,a,y,2} \sim \text{Normal}(0, \sigma^2_{j,2})$; and the subscript 2 is used to separate the term from the one in M1. We used $\text{Normal}(0, \sigma^2)$ to represent the normal distribution and to avoid confusion with population size N. By modelling $N_{j,a,y}$ using a distribution (with median $N_{a,y}$), the possible heterogeneity of the population density in each survey location, $\varepsilon_{j,a,y,N} \sim MVN(0, \sigma^2_{y,a,N,2})$, is modelled. The subscript 2 in $\sigma^2_{y,a,N,2}$ again is used to separate the term from the one in M1 and MVN means multivariate normal distribution. This model is also called a nested random effect model and it has been applied successfully in many studies (Banerjee *et al.,* 2003; Lawson *et al.,* 2003; Waller and Gotway, 2004); however, the correlation among surveys is rather "all or nothing" as responses on either side of a survey boundary are assumed to be uncorrelated. The random effect model allows the temporal variation of the spatial heterogeneity shown as spatial synchrony/asynchrony to be modelled. The inverse Wishart distributions are used as the conjugate prior for the covariance matrix of the multivariate normal distributions and were used here. Priors used in this model are listed in Table 1.

There have been studies that suggest fish distributions and abundance are spatially autocorrelated because of autocorrelated environmental factors or dispersal (Simard *et al.,* 1992; Cressie, 1993; Petitgas, 1993, 2001; Addis *et al.,* 2009). Modelling spatial autocorrelation has been used to adjust for autocorrelation when standardizing catch rate (Nishida and Chen, 2004). Our third model under consideration is a conditional autoregressive (CAR) model. The CAR provides a method to model the spatial autocorrelation of different surveys by introducing a set of spatially correlated multivariate normal random effects in the model to account for spatial correlation (SCA_CAR **M3**), i.e.

$$\begin{aligned} \text{Ln}(I_{j,a,y}) &= \text{Ln}(q_{j,a}N_{a,y}) + \varepsilon_{j,a,y,3} + \varepsilon_{j,a,y,4} \\ \varepsilon_{j,a,y,4} &\sim N(\bar{\varepsilon}_{j,4}, \sigma^2_{j,4}/n_j) \\ \bar{\varepsilon}_{j,4} &= \sum_{k \in \text{neighbor}(j)} w_{j,k}\varepsilon_k/n_j. \end{aligned} \tag{3}$$

In this model, the $\varepsilon_{j,a,y,3}$ are treated as independent and identically distributed among different surveys, $\varepsilon_{j,a,y,3} \sim \text{Normal}(0, \sigma^2_{j,3})$, and $\varepsilon_{j,a,y,4}$ are viewed as correlated, with the size of the correlation depending on the locations of the surveys and their neighbours. The variable ε_k is the error term of the kth neighbour of survey j. Subscripts 3 and 4 in $\varepsilon_{j,a,y,3}$ and $\varepsilon_{j,a,y,4}$ are used to represent the differences in index uncertainty in this model and to separate them from similar terms in M1 and M2. The variable n_j is the number of neighbours for survey j. Here, the sum of $\varepsilon_{j,a,y,4}$ is always zero; only correlations among neighbouring surveys were counted and neighbours were weighted equally. Priors used in this model are listed in Table 1.

The fourth model that we considered is close to M3, but we modelled the covariance of the correlated surveys according to the distances among them, i.e. both neighbouring surveys and non-neighbouring surveys were considered to be correlated (SCA_Distance **M4**),

$$\begin{aligned} \text{Ln}(I_{j,a,y}) &= \text{Ln}(q_{j,a}N_{a,y}) + \varepsilon_{j,a,y,5} + \varepsilon_{j,a,y,6} \\ \varepsilon_{j,a,y,6} &\sim \text{MVN}(0, V), \end{aligned} \tag{4}$$

where $\varepsilon_{j,a,y,5} \sim \text{Normal}(0, \sigma^2_{j,5})$ and V is the variance–covariance matrix of the normally distributed but spatially correlated $\varepsilon_{j,a,y,6}$. Subscripts 5 and 6 in $\varepsilon_{j,a,y,5}$ and $\varepsilon_{j,a,y,6}$ are used to represent the differences of uncertainty of indices in this model to separate them from similar terms in M1 to M3. If g and h represent two survey locations, then the respective errors should be ε_g and ε_h. The covariance $\text{Cov}(\varepsilon_g, \varepsilon_h)$ between ε_g and ε_h is a function of the distance d_{gh} between g and h, and of the range H (i.e. the maximum distance over which any significant autocorrelation

Table 1. Priors used in the models (catches are in 10^6 fish in the models).

Models	Scenarios	Parameters and their priors
M1 A commonly used SCA model; the abundance indices are independent and proportional to population abundance	S1	$\sigma_c^2 \sim U(0.001, 10)$; $\sigma_j^2 \sim U(0.001, 1)$; $\sigma_R^2 \sim U(0.001, 10)$; $\bar{N}_{a>1,y=1982} \sim U(1, 100) \times C_{a,y=1982}$; $\sigma_N^2 \sim U(0.001, 10)$; $F_y \sim U(0.001, 2)$; $S_a \sim U(0, 1)$; $\mathrm{Ln}(\bar{R}_y) \sim U(\min(\mathrm{Ln}(C_{1,y=1982:2007})), \max(\mathrm{Ln}(100C_{cohort,y})))$; $\mathrm{Ln}(q_{j,a=1}) \sim U(\mathrm{Ln}[\min(I_{j,a=1}/\text{upper bound of } \bar{R})], \mathrm{Ln}[\max(I_{j,a=1}/\text{lower bound of } \bar{R})])$; $\mathrm{Ln}(q_{j,a>1}) \sim U(\mathrm{Ln}[\min(I_{j,a>1,y}/100C_{a>1,y})], Ln[\max(I_{j,a>1,y}/C_{a>1,y})])$
	S2	Same as M1S1 but $\sigma_c^2 \sim U(0.001, 1)$; $\sigma_j^2 \sim U(0.001, 0.5)$; $\sigma_N^2 \sim U(0.001, 5)$; $\mathrm{Ln}(R_y) \sim U(0, 200)$; $\mathrm{Ln}(q_{j,a}) \sim U(-8, 4)$
M2 A spatial SCA model with abundance indices modelled as random effect	S1	Same as in M1S1, but also $\sigma_{j,2}^2 \sim U(0.001, 1)$; $\varepsilon_{j,a,y,N}$ for aged indices $j \sim MVN(u_2, V_2)$, $\mu_2 = [0, 0, 0, 0, 0, 0]$; $1/V_2 = dwish(R, k)$; $k = 9$; $R = [\ ]_{6\times6}$ with main diagonal values = 0.1; and other values = 0.005; $\varepsilon_{j,a,y,N}$ for non-aged indices $j \sim MVN(u_3, V_3)$, $\mu_3 = [0, 0, 0, 0, 0, 0, 0, 0]$; $1/V_3 = d\mathrm{wish}(R', k')$; $k' = 11$; $R' = [\ ]_{8\times8}$ with main diagonal values = 0.1; and other values = 0.005
	S2	Same as in M2S1, but $\sigma_{j,2}^2 \sim U(0.001, 0.5)$ $R = [\ ]_{6\times6}$ with main diagonal values = 0.05; and other values = 0.001; $R' = [\ ]_{8\times8}$ with main diagonal values = 0.05; and other values = 0.001
M3 A spatial SCA model with correlations among neighbouring surveys modelled as conditional autoregressive process	S1	Same as in M1, but also $\sigma_{j,3}^2 \sim U(0.001, 1)$; $\sigma_{j,4}^2 \sim U(0.001, 1)$; $\varepsilon_k \sim U(0.001, 10)$;
	S2	Same as in M1, but also $\sigma_{j,3}^2 \sim U(0.001, 0.5)$; $\sigma_{j,4}^2 \sim U(0.001, 0.5)$; $\varepsilon_k \sim U(0.001, 5)$;
M4 A spatial SCA model with abundance indices assumed to be spatially autocorrelated and correlation modelled as a function of distance between surveys	S1	Same as in M1, but also $\sigma_{j,5}^2 \sim U(0.001, 1)$; $\sigma_{j,6}^2 \sim U(0.001, 1)$; $1/H \sim U(0.2, 2)$;
	S2	Same as in M1, but also $\sigma_{j,5}^2 \sim U(0.001, 0.5)$; $\sigma_{j,6}^2 \sim U(0.001, 0.5)$; $1/H \sim U(0.2, 2)$
	S3	Same as in M1, but also $\sigma_{j,5}^2 \sim U(0.001, 1)$; $\sigma_{j,6}^2 \sim U(0.001, 1)$; $1/H \sim U(0.25, 2)$;

See text for the justification of the priors.

occurs), as specified by the longitude and latitude of the samples, i.e. $\mathrm{Cov}(\varepsilon_g, \varepsilon_h) = {\sigma_6}^2 f(d_{gh}, H)$. The variable ${\sigma_6}^2$ is the base covariance when the distance is 0 and the covariance model used is an exponential model, $f(d_{gh}, H) = \exp(-d_{gh}/H)$. Here, instead of using the longitude and latitude to determine the distance between surveys, we used the number of states between g and h as the distance. For example, MD and DE are neighbours in Figure 1, and the distance between surveys in these 2 states is defined to be 1; MD and NY are not neighbours since DE and NJ are between them, hence the distance between surveys in MD and NY is 3. Priors used in this model are listed in Table 1.

Both M3 and M4 assume that spatial autocorrelation may cause spatial heterogeneity, but their modelled heterogeneity does not vary over time. M2 allows the modelled spatial heterogeneity to vary over time, i.e. allows for spatial asynchrony (Buonaccorsi *et al.*, 2001; Banerjee *et al.*, 2003).

Bayesian approach and priors

We used a Bayesian approach to fit the spatial hierarchical models to data collected from different sources (Banerjee *et al.*, 2003; Calder *et al.*, 2003). Because models M2 to M4 model I hierarchically, the posterior density distribution for parameters needs to consider hyperpriors related to I. A Bayesian model (M1) defines the posterior density for parameters $(p(\theta = \bar{R}, \bar{N}_{a>1,1982}, F_y, S_a, q_{j,a}, \sigma_j, \sigma_c, \sigma_R, \sigma_N | C, I))$ using Bayes' theorem as

$$p(\theta|C, I) \propto L(I|N, q, \sigma_j) L(C|N, F, S, \sigma_c) \pi(\theta), \tag{5}$$

where $L(I|N, q, \sigma_j)$ equals $\prod_y \prod_a \prod_j g(I_{j,a,y}|N_{a,y}, q_{j,a}, \sigma_j)$, which is the likelihood function of I (all the available relative abundance indices). The variable $L(C|N, F, S, \sigma_c)$ equals $\prod_y \prod_a h(C_{a,y}|N_{a,y}, F_y, S_a, \sigma_c)$, which is the likelihood function of C; and $\pi(\theta)$, the prior of the parameters, equals $\prod_y \prod_a \prod_j \pi(\bar{R}) \pi(\bar{N}_{a>1,1982}) \pi(F_y) \pi(S_a) \pi(q_{j,a}) \pi(\sigma_j) \pi(\sigma_c) \pi(\sigma_R) \pi(\sigma_N)$.

In models M2 to M4, assigning priors for hyperparameters is also needed to calculate the joint posterior. For example when M2 is used, the joint posterior is

$$p(\theta = \bar{R}, \bar{N}_{a>1,1982}, F_y, S_a, q_{j,a}, \sigma_{j,2}, \sigma_c, \sigma_R, \sigma_N, \sigma_{N,2}|C, I) \propto L(I|N, q, \sigma_j)L(C|N, F, S, \sigma_c)\pi(\theta), \tag{6}$$

where $L(I|N, q, \sigma_j)$ is the likelihood function of I (all the available relative abundance indices) and is calculated as $L(I|N, q, \sigma_j) = \prod_y \prod_a \prod_j g(I_{j,a,y}|N_{j,a,y}, q_{j,a}, \sigma_{j,2})$. The variable $L(C|N, F, S, \sigma_c)$ is the likelihood function of C and is calculated as $L(C|N, F, S, \sigma_c) = \prod_y \prod_a h(C_{a,y}|N_{a,y}, F_y, S_a, \sigma_c)$, and $\pi(\theta)$ is $\prod_y \prod_a \prod_j \pi(\bar{R})\pi(\bar{N}_{a>1,1982})\pi(F_y)\pi(S_a)\pi(q_{j,a})\pi(\sigma_{j,2})\pi(\sigma_c)\pi(\sigma_R)\pi(\sigma_N)\pi(\sigma_{N,2})$.

In the equations above, $g(I_{j,a,y}|\ldots)$ is the probability density function for $I_{j,a,y}$ with parameters $N_{a,y}, q_{j,a}, \sigma_j$ or $N_{a,y,j}, q_{j,a}, \sigma_{j,2}$; $h(C_{a,y}|\ldots)$ is the probability density function of $C_{a,y}$ given parameters $N_{a,y}, F_y, S_a, \sigma_c$; $f(N_{a,y,j}|N_{a,y}, \sigma_{a,y,N,2})$ is the probability density function of $N_{a,y,j}$ with parameters $N_{a,y}, \sigma_{a,y,N,2}$. The same algorithm can be used to develop the joint posterior for M3–M4.

Priors need to be specified for all the parameters in a Bayesian analysis. Usually two types of prior distributions are used in a Bayesian analysis: non-informative and informative (Berger, 1985; Gelman *et al.*, 2004; Gelman, 2006). The choice of a non-informative or informative prior for a parameter was determined by the reliability and details of prior knowledge. Priors that are vaguely informative were explained in the model section above. All the priors for the variances for recruitment, catch, and abundance indices are non-informative, and wide uniform distributions were used (Table 1).

A critical issue in using Markov Chain Monte Carlo (MCMC) methods is the convergence diagnostic for the posterior distribution (Cowles and Carlin, 1996). Here, we monitored the trace for key parameters, and also used the Gelman and Rubin statistic (Gelman and Rubin, 1992; Spiegelhalter *et al.*, 2004). Three chains were used. The three chains converged after 20,000 iterations with a thinning interval of 5 based on the convergence criteria. The initial iterations were discarded. The posterior distributions of the key parameters were obtained through a kernel smoothing approach (Bowman and Azzalini, 1997).

Simulation study

After the study based on the example fishery was complete, a simulation study was conducted to test the performance of the proposed models and evaluate the model selection uncertainty when inference was based on a model selection criterion (here Deviance Information Criterion, DIC, see below). Model selection uncertainty increases when the "true" model cannot be found based on the model selection criteria, a phenomenon that has been found to be very common in dealing with ecological and fisheries data (Draper, 1995; Burnham and Anderson, 2002; Jiao *et al.*, 2008). Such a simulation study helps us to understand how robust the recommended model is, how high the model selection uncertainty is, given the example fishery, and allows evaluation of the performance of the recommended model even when the true model cannot be found based on the model selection criteria (Draper, 1995; Jiao *et al.*, 2008). The following simulation algorithm was used to: (i) estimate recruitment, fishing mortality, and all the other parameters from the models (M1—M4) using data of the example fishery and treat these estimates as the "true" population dynamics parameters; (ii) generate population abundance indices data and catch-at-age data from a Monte Carlo simulation based on estimated "true" recruitment, fishing mortality, selectivity and uncertainty levels equivalent to the uncertainties estimated from the original "true" population; (iii) analyse the generated dataset using the four models; and (iv) evaluate the uncertainty arising from model selection and the performance of the "best" model selected by the model goodness of fit (DIC here) based on the relative estimation error (*REE*) and absolute relative estimation error (*AREE*, see Table 2 for the simulation design). Steps (2) through (4) above were repeated 100 times to

Table 2. Relative estimation bias (*REE*) of fishing mortality (*F*), selectivity (*S*) and recruitment (*R*), and the probability of being the best model of 100 simulation runs.

Scenarios	True model used in the simulation	Model used for estimation	Probability of being the best model	Mean of *REE* of *F*	Mean of *REE* of *S*	Mean of *REE* of ln(*R*)	Mean of *AREE* of *F*	Mean of *AREE* of *S*	Mean of *AREE* of ln(*R*)
S1	M1	M1	0	−3.79	2.70	1.21	18.26	11.46	5.37
		M2	100	−3.97	2.28	1.33	17.65	11.67	5.27
		M3	0	−2.76	5.06	1.93	18.54	11.46	5.98
		M4	0	−4.26	2.27	1.20	17.48	11.57	5.15
		Best Model		−3.97	2.28	1.33	17.65	11.67	5.27
S2	M2	M1	0	−5.10	0.72	3.47	15.36	8.60	11.02
		M2	100	−3.89	0.54	2.64	14.23	8.66	7.11
		M3	0	−5.21	2.71	4.12	16.93	8.72	13.68
		M4	0	−4.34	−0.51	3.13	14.25	8.93	9.27
		Best Model		−3.89	0.54	2.64	14.23	8.66	7.11
S3	M3	M1	0	−3.52	4.50	−0.18	25.35	13.64	6.16
		M2	100	−2.53	0.87	−0.35	19.85	11.56	5.46
		M3	0	−4.46	5.62	−0.06	17.99	11.32	4.97
		M4	0	−3.46	2.51	−0.55	22.62	13.66	5.80
		Best Model		−2.53	0.87	−0.35	19.85	11.56	5.46
S4	M4	M1	40	−4.15	3.36	1.57	17.54	10.22	5.55
		M2	60	−3.80	2.84	1.70	17.26	10.16	5.43
		M3	0	−3.14	5.58	2.02	17.26	10.85	6.74
		M4	0	−4.22	2.59	1.49	16.90	10.44	5.19
		Best Model		−3.89	3.02	1.63	17.36	10.20	5.42

yield 100 sets of estimated population growth rates and population densities from each model.

The *REE* and *AREE* statistics which have been widely used in fisheries, are used here to compare the bias accuracy and precision in the corresponding parameter estimates when different models are used (Schnute, 1987; Jiao *et al.,* 2009a, b). The variable $REE(\hat{F}_i)$ for estimated fishing mortality rate in year y, $\hat{F}_y$, was calculated as follows:

$$REE(\hat{F}_i) = \frac{1}{n}\sum_{y} \frac{\hat{F}_{y,i} - F'_y}{F'_y} \times 100$$
$$AREE(\hat{F}_i) = \frac{1}{n}\sum_{y} \frac{|\hat{F}_{y,i} - F'_y|}{F'_y} \times 100, \qquad (7)$$

where i indicates the ith simulation run and n is the number of the years. The variable F'_y is the true fishing mortality rate in year y, and $\hat{F}_{y,i}$ is the estimated fishing mortality in year y in the ith simulation. An estimation procedure with small *REE* suggests that it performs well and tends to have smaller bias in estimating *F*. A small AREE suggests that the approach performs better and tends to have better precision in estimating *F*. The same approach was used to estimate *REE* and *AREE* for recruitment and selectivity.

Model selection uncertainty was evaluated through a probability of choosing the "true" model as the best model, based on the lowest DIC value. For example, when the M1 model was used as the true model, in each of these 100 runs, the simulation algorithm would pick the best model based on the DIC values (smallest DIC means the best model); the best model would be recorded in each of the simulation runs. After the 100 runs, the proportion of times each model was chosen as the best model was calculated based on the DICs of each model in the 100 runs. For example, if the M1 model was chosen as the best model in 20 of 100 runs, then the probability is 20%. In this simulation, the results of the *REE*s and *AREE*s, and the probability of being selected as the best model, from the first 50 runs and the second 50 runs were similar. This indicated that the simulation results were stable for *REE* and *AREE*, and for model selection uncertainty estimation. We then decided to use 100 runs considering the long time for computation (Schnute, 1987; Jiao *et al.,* 2008, 2009a, b).

Model goodness of fit

The goodness-of-fit statistics for the hierarchical spatially structured Bayesian statistical catch-at-age (SBSCA) models were compared with the classical, nonspatial SCA model based on the estimates of the DIC:

$$DIC = 2\bar{D} - \hat{D} or \bar{D} + p_D$$
$$D(x, \theta) = -2 \log \text{Likelihood}(x|\theta) \qquad (8)$$
$$p_D = \bar{D} - \hat{D},$$

where *D* is the deviance, a measurement of how well each model fits the observed data, p_D is the effective number of parameters in a Bayesian model, $\bar{D}$ is the posterior mean of the deviance, and $\hat{D}$ is the deviance of the posterior mean. Here, x includes $C_{a,y}$, $I_{j,a,y}$ and θ includes $\bar{R}$, $\bar{N}_{a>1,1982}$, F_y, S_a, $q_{j,a}$, σ_j, σ_c, σ_R, σ_N in the SCA model and also includes hyperparameters used in the distribution of the indices in the other three models, such as parameters in the Wishart (*d*wish, in Table 1) distribution, and *H* in the exponential autocorrelation function. The DIC is a hierarchical modelling generalization of AIC (Akaike information criterion) and BIC (Bayesian information criterion). The lower the DIC value, the better the model. It is particularly useful in hierarchical Bayesian model selection problems (Spiegelhalter *et al.,* 2002 2004; Jiao *et al.,* 2008, 2009a, b, 2010).

Retrospective analysis

Retrospective error has been one of the important issues in fisheries stock assessments (Mohn, 1999; NEFSC, 2008). An extra 3-year retrospective analysis was done for each of the models. The retrospective pattern was treated as one of the two criteria to compare models. Here, 1 year retrospective error was measured as follows:

$$E1_t = \frac{(N_t|_{\text{data to year } t} - N_t|_{\text{data to year } t+1})}{(N_{\text{data to year } t+1})}, \qquad (9)$$

where $N_t|_{\text{data to year } t}$ is the estimated population abundance in year t when data up to year t was used in the model (Jiao *et al.,* 2012). The second criteria is based on Mohn (1999), and it is calculated as below for the 3-year retrospective analysis:

$$E2 = \sum_{t=2007-5}^{2007} \frac{N_t|_{\text{data to year } t} - N_t|_{\text{data to year 2007}}}{N_t|_{\text{data to year } t}}. \qquad (10)$$

Sensitivity analysis

In this analysis, non-informative priors were primarily used. Our preliminary analysis found that using an informative prior for parameters tended to decrease the computing time and the Markov Chains converged much faster. This characteristic of an MCMC is very important for models that are as complicated as the ones developed here. We then developed a sensitivity analysis using informative priors for the variance terms, σ^2. The informative prior for σ^2 was based on the modelling analysis from M1 to M4, i.e. two times the variance of model M_i, $\sigma^2|_{M_i}$, was used as the prior of the second scenario of each model. The use of priors from previous analyses has been suggested as valuable in Bayesian analysis (Gelman *et al.,* 2004). This can be a useful way to elicit informative priors. Here we widened the before two times the variance of model M_i, $\sigma^2|_{M_i}$, for the prior of σ^2 in model M_i to make sure that the prior was not too restrictive. For the spatial models we added extra scenarios to test the appropriateness of the priors for the variance–covariance matrix of the spatially correlated residuals. Details of the priors in the sensitivity analysis are presented in Table 1.

Results

Our MCMC convergence diagnostic based on the Gelman and Rubin statistic and the trace plots showed that convergence of the MCMC algorithm for all models are guaranteed. The Gelman and Rubin statistic for all parameters, including all variance terms, ranged from 0.99 to 1.01, indicating convergence of the Markov chains. We also visually observed the trace plots of the major parameters, which showed good mixing of the three chains, also indicative of convergence of the MCMC chains (figures not shown). For the simulation runs, only the Gelman and Rubin statistic was used as the tool to diagnose convergence of the MCMC, and runs with Gelman and Rubin statistic beyond the range of 0.99–1.01 were discarded. Extra simulation runs were added in such cases (only observed in 2 of the 100 runs for M4).

Extending the commonly used SCA model (SCA, M1) to a hierarchical spatial random effect model (SCA_RE, M2) increased the

Table 3. DIC and retrospective error estimates when different models are used.

Models	**Scenarios**	**DIC**	E_{2004}	E_{2005}	E_{2006}	$E2$
M1	S1	2437.6	0.24	0.01	0.34	0.57
	S2		0.23	−0.07	0.15	0.33
M2	S1	2140.2	0.12	−0.03	0.34	0.66
	S2		0.06	−0.01	0.26	0.43
M3	S1	2764.5	0.16	−0.01	0.34	0.53
	S2		0.22	0.02	0.36	0.62
M4	S1	2467.6	0.31	0.03	0.44	0.81
	S2		0.28	0.06	0.38	0.73
	S3		0.35	0.05	0.42	0.83

E_{year} is the retrospective error for the given year (see text for explanation), and $E2$ is the retrospective error used in Mohn (1999).

model goodness-of-fit dramatically. The difference between DICs from these two models was 297.4 (Table 3). However, the SCA_CAR model (M3) decreased model goodness-of-fit (Table 3). The spatial hierarchical SCA_Distance model, that assume that covariance among surveys is a function of their distance (M4), also resulted in a relatively higher DIC than when M1 was used but not as high as when M3 was used. The differences between the DIC values indicated that modelling spatial synchrony/asynchrony through hierarchical spatial models is valuable (M2 has the lowest DIC value). Because the fit for M3 and M4 was much worse than M1, spatial autocorrelation among neighbouring areas as modelled in M3 or by M4 (using the distance between locations) seems not evident. Comparison among DICs suggested that M2 was the most appropriate model and that the weakfish population

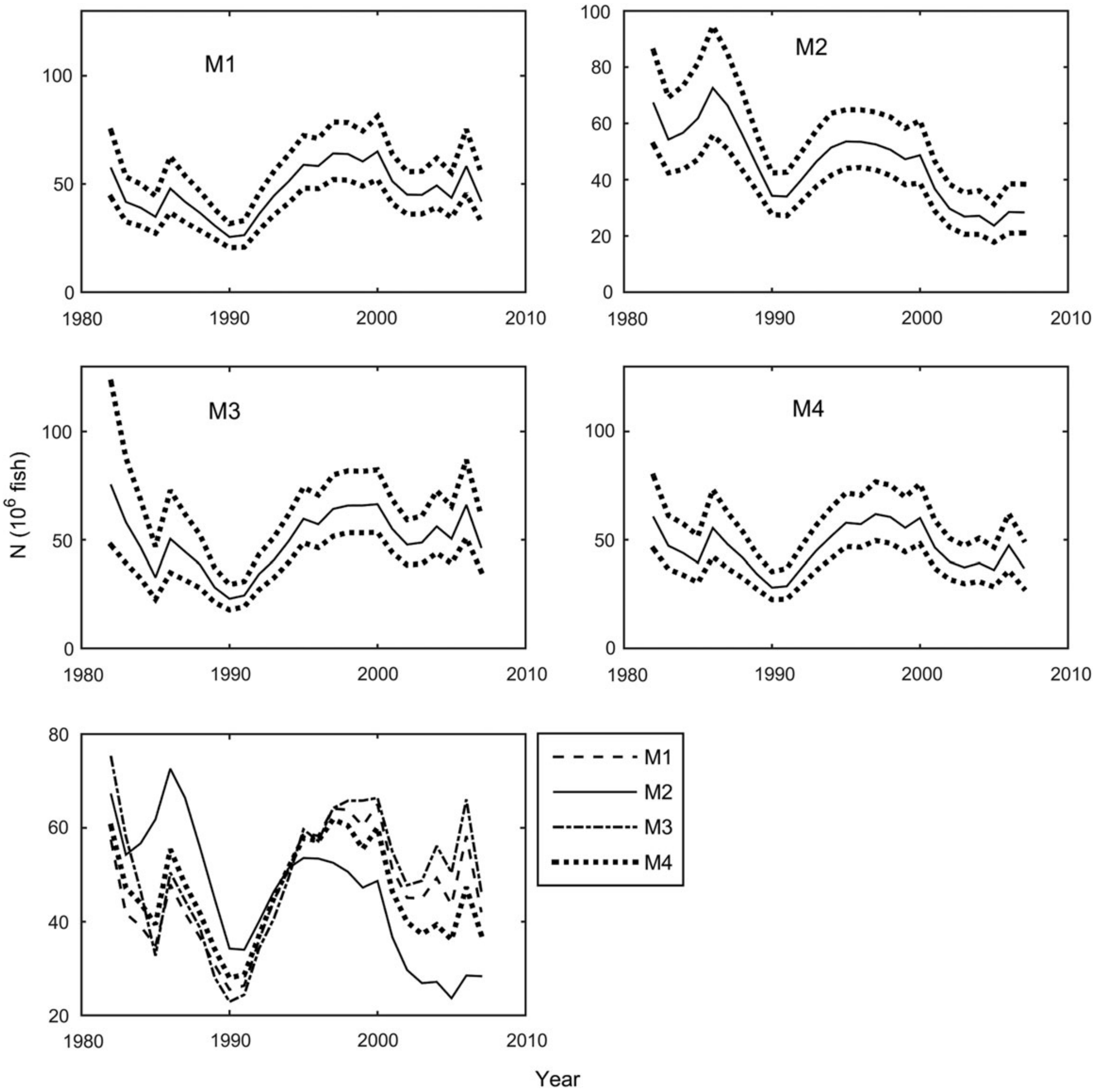

Figure 2. Estimated posterior population abundance. Continuous line represents mean estimates, and dotted lines represent 95% credible intervals.

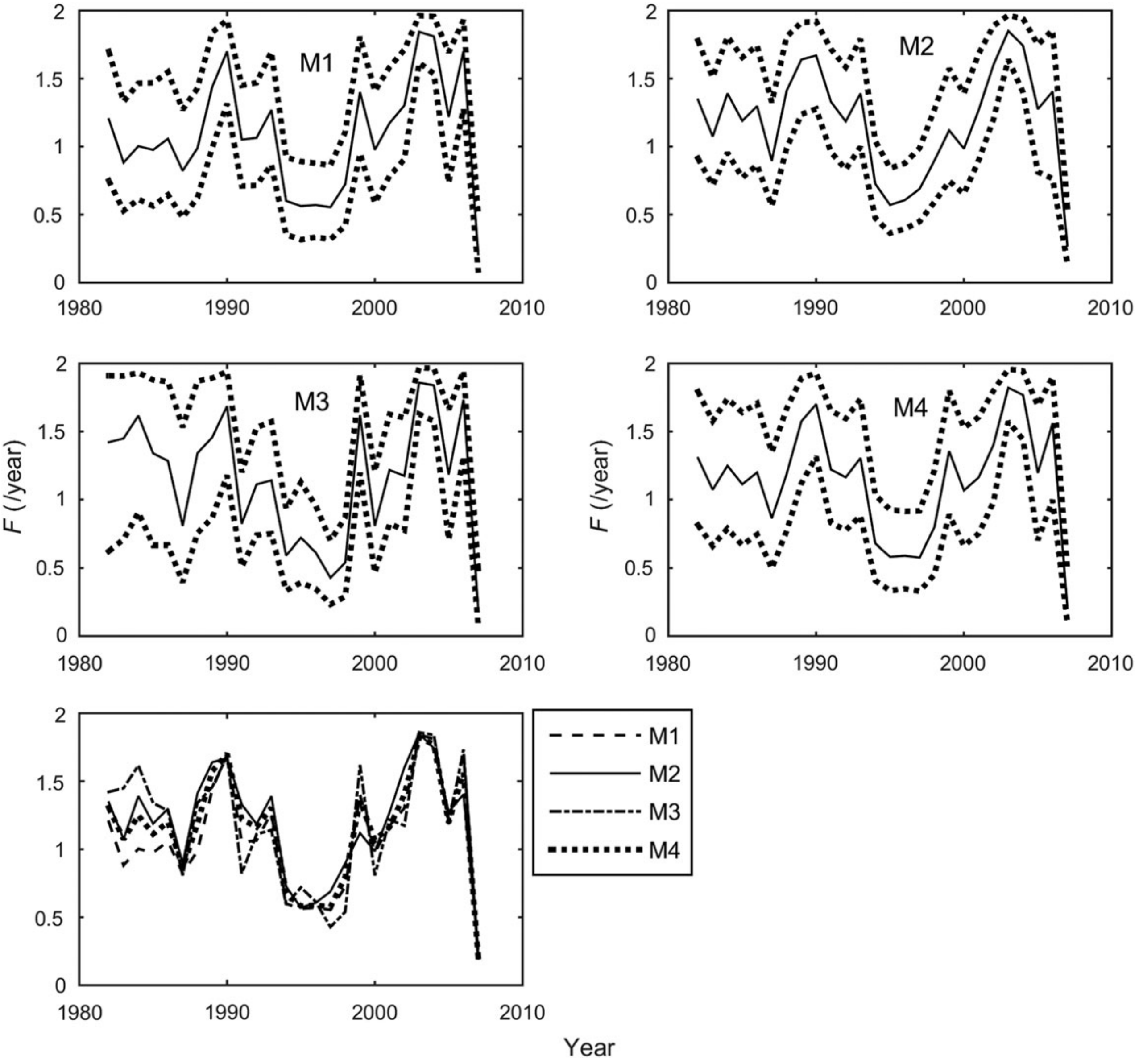

Figure 3. Estimated posterior fishing mortality. Continuous line represents mean estimates, and dotted lines represent 95% credible intervals.

distribution is highly heterogeneous as reflected in the random effect in different surveys and has spatial asynchrony over time.

The estimated population trends from the four models were not the same, with results from M1, M3, and M4 being much closer (Figure 2). M2 resulted in lower population size after the mid-1990s than M1, M3 and M4. Fishing mortality estimation followed similar patterns when different models were used (Figure 3). Here although all the models were calibrated using the same relative abundance indices, expected trends in population size can be different because of the different functions of the abundance indices equations used in the spatial hierarchical models.

The spatial synchrony/asynchrony was modelled as a random effect in the surveys in M2. The estimated $\varepsilon_{j,a,y,2}$ values were plotted to show the spatial heterogeneity and its variation in M2. Bubble plots (Figure 4) were used to represent the spatial variation among surveys with positive $\varepsilon_{j,a,y,2}$ plotted in red and negative values of them plotted in blue. Positive values indicate that the corresponding survey locations tend to have higher population densities than average over time, while negative values indicate that the corresponding locations tend to have lower population densities than average over time. This pattern is associated with synchrony among some surveys/locations and asynchrony with other surveys/locations. The NMFS survey and SEAFALL tended to have a higher than average population densities for ages 2–5 after 2003 although the proportions of ages 2–5 fish are low in both surveys (Figure 4A). DEDFG, NJDEP, and MRFSS surveys tended to have lower than average population densities after 2003. DWDFG and NJDEP tended to have to higher than average population densities from mid-1990s to 2003.

Spatial synchrony/asynchrony of YOY was clearly reflected in the results of M2. The random effects from the YOY surveys indicated that the density of the population was probably changing in different survey locations over time (Figure 4B). The DEDFW, NCDMF, VIMS survey, and RI surveys tended to have higher than average

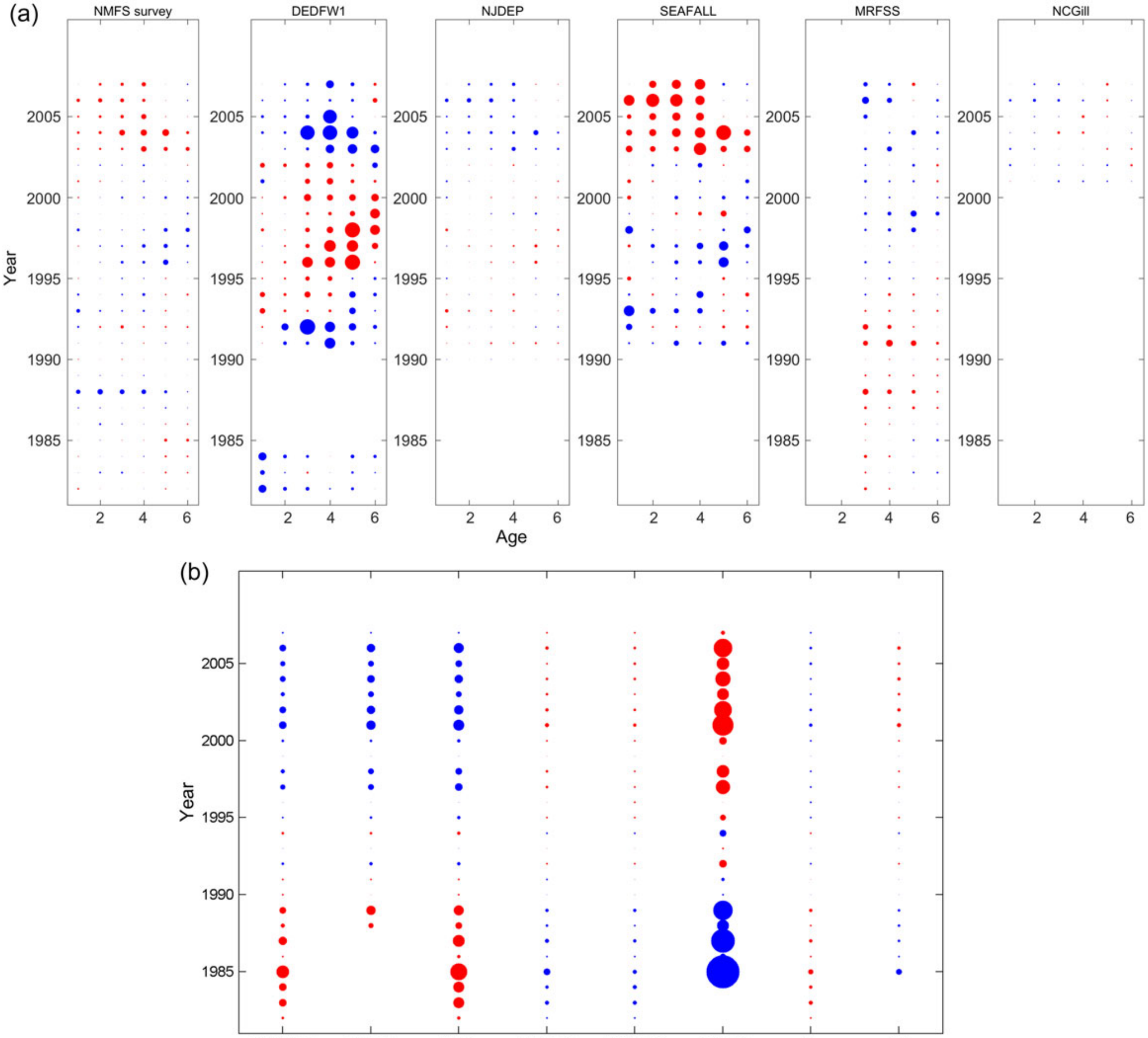

Figure 4. Spatial heterogeneity reflected from different surveys shown as differences from the mean population size M2. Positive values were plotted in red, while negative values were plotted in blue. See text or the explanation of the bubble plot. (a) Spatial-temporal variation of the fish groups shown from 6 age surveys. See Supplementary Table S1 for the explanation of the surveys. See text for the explanation of the bubble plot. (b) Spatial-temporal variation of the age 1 fish groups shown from 8 YOY surveys. See Supplementary Table S1 for the explanation of the surveys.

YOY populations before 1990, but had lower than average YOY population after 1995. The change in the YOY population density was in contrast to the trend for MDDNR1, MDDNR2, and CT surveys, that showed lower than average YOY populations before 1990 but higher than average populations after 1995. The period of 1990–1995 seemed to be the time where the change happened.

The estimated posterior distributions of N_{msy} and F_{msy} from M1 and M3 were similar but different for M2 and M4 (Figure 5). M2 resulted in smaller F_{msy} and larger N_{msy} whereas M4 resulted in larger F_{msy} and smaller N_{msy}.

Model selection uncertainties from the simulation study were high. With the example stock, probabilities of determining the true model were, respectively, 0, 100, 0, and 40% for the M1–M4 models (Table 2). However, the simulation study also showed that the "true" model tended to give the estimate with lower to lowest *REE* and *AREE* values, which means that the parameter estimates are better, but not always the best (Table 2). The *REE* and *AREE* values calculated from the "best model" selected based on DIC, were low and very close to the *REE* and *AREE* calculated when the true models were used (Table 2). This implies that the DIC works well in selecting models among these SCAs (Jiao *et al.,* 2009a, b).

Discussion

Spatial synchrony/asynchrony often exists among species of interest because of autocorrelated ecological variables, species dispersal, species interaction, and collared noises of the environment, and may cause serious errors in data analyses if neglected (Legendre, 1993; Heino *et al.,* 1997; Vasseur, 2007; Pandit *et al.,* 2013). Studies that incorporate spatial processes into fishery data analysis were limited to surveys on either abundance or relative abundance,

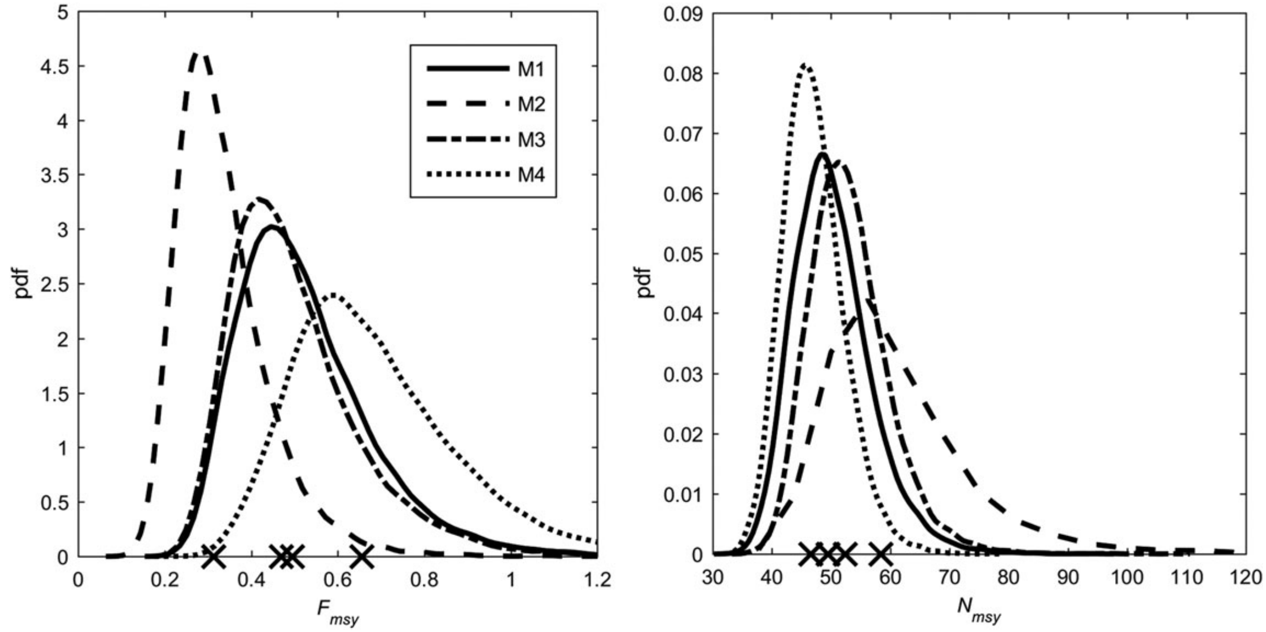

Figure 5. The estimated maximum sustainable population abundance *Nmsy* and maximum sustainable fishing mortality *Fmsy*. Markers x are the median of the posterior distributions.

i.e. the studies either estimate the abundance based on the survey data directly, or use the catch rate standardization to develop relative abundance based on the surveys (Petitgas, 1993, 2001; Nishida and Chen, 2004; Addis *et al.*, 2009). In an age-structured model, the spatial synchrony/asynchrony can be reflected in surveys from different states and regions. The method to integrate different surveys from different locations into a stock assessment model as we propose here is largely needed and has not been developed previously. Our study suggests that our proposed spatial hierarchical Bayesian statistical catch-at-age models can be a very useful and novel method to incorporate spatial synchrony and asynchrony over time into a fisheries stock assessment.

Three hypotheses about the possible spatial dynamics of the population distribution/density were modelled and tested through model comparison. The largely reduced DIC values using the spatial hierarchical model (M2 here) suggested that incorporating spatial variation of the population abundance is worthwhile. It also suggested that spatial asynchrony of Atlantic weakfish is obvious and hence needs to be taken into account by the model. However, the partial correlation structures tested in M3 and M4 did not improve model fit. The increased DIC values using M3 and M4 suggested that spatial heterogeneity of Atlantic weakfish is probably less continuous (M4) and less influenced by the neighbouring regions (M3). This could be derived from the fact that the differences in abundance among location are completely random (M2) or because the real spatial structure is different from those tested in M3 and M4. Other functions, such as spherical and Gaussian models, may be considered in the future (Rossi *et al.*, 1992; Heino *et al.*, 1997).

The spatial hierarchical model that fit the weakfish data the best (M2) suggested that the spatial synchrony and asynchrony among surveys over time was changing around the mid-1990s and early 2000s. After entering the 2000s Atlantic weakfish tended to have a density that was higher during this period than before in the southern area and in the offshore area. According to the time-series surveys on catch of weakfish from private boats by recreational anglers, both the ocean catches and inland catches increased in the South-Atlantic in recent years, but decreased in recent years in the Mid-Atlantic area. The ocean catches in the 1980s in the Mid-Atlantic area are not less than those from inland in the Mid-Atlantic area but are much lower in the South-Atlantic area (Figure 6). These catch observations are consistent with our modelling results on spatial asynchrony.

Results from both prior scenarios when the same models were used were similar, which indicated that the informative priors for variances are appropriate for future stock assessment. The stability of the results might be a result of the hierarchically structured variances (Gelman *et al.*, 2004). Hierarchical models have been found to provide robust estimates of the parameters in models in a variety of areas, such as pharmaceutical, ecological, and fisheries (Gelman *et al.*, 2004; Jiao *et al.*, 2009a, b, 2011).

In our simulation study, we found that the estimated posterior means of the parameters were close to the "true" values in most of the runs. We also found that the *DIC* recommended models resulted in parameter estimates with lower estimation uncertainty that tend to be close to the estimates when the "true" models were used. Schnute (1987) and Jiao *et al.* (2008, 2009a, b) found that the model selection uncertainty can be rather high, and the models recommended by the information based criteria have low probability of being the "true" model. This discrepancy suggested that the model selection uncertainty is probably less when the ΔDIC is higher and $\Delta DIC/DIC$ is larger.

Our study investigated possible spatial hypotheses based on the example fishery and provides potential models that could be used to account for spatial synchrony and asynchrony. We recommend that the preferred model be considered as an operational model for future stock assessment of the example fishery. Other hypotheses on

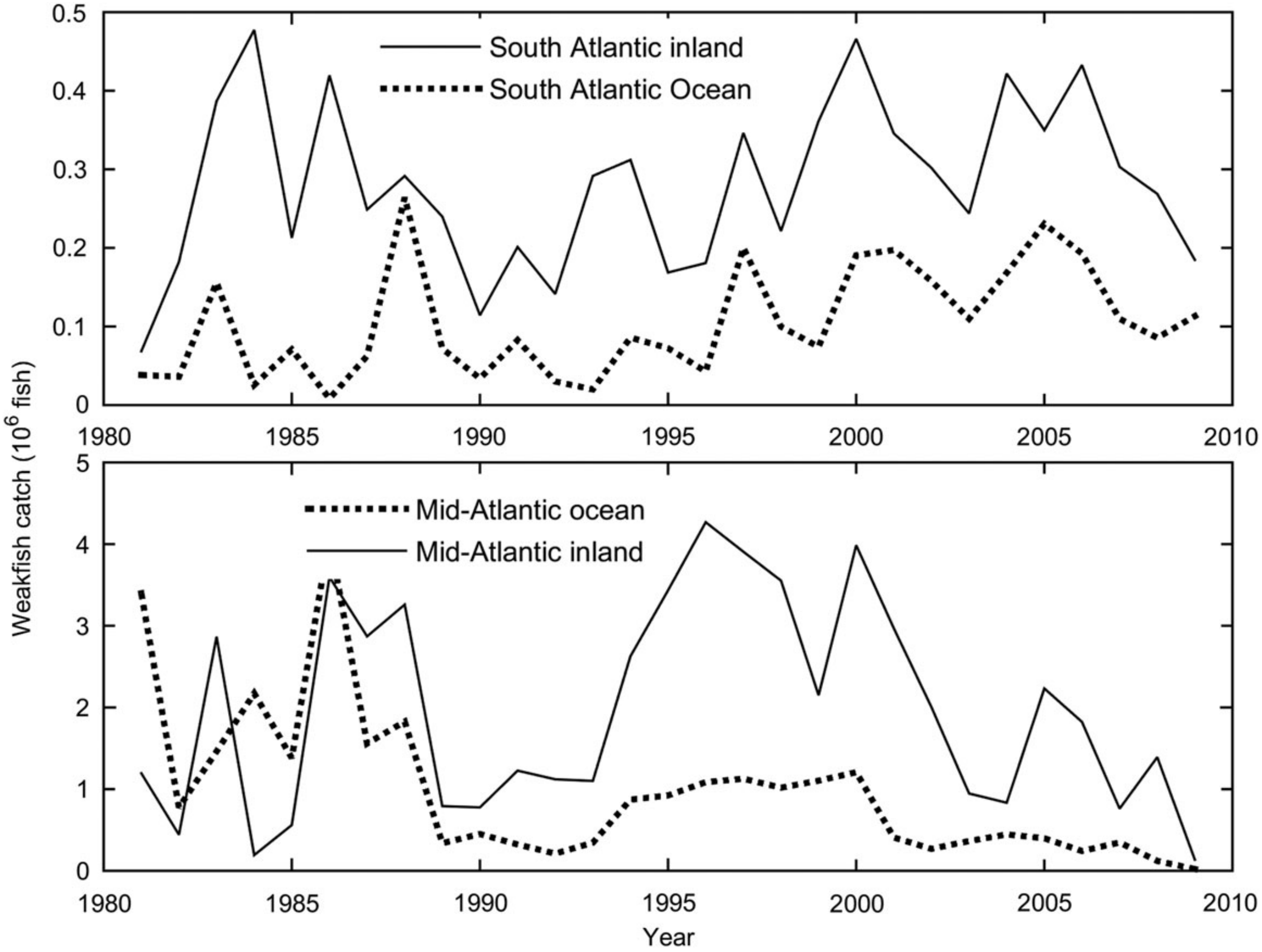

Figure 6. A time-series survey of private boat (only) catch of weakfish by recreational anglers for the Midand South-Atlantic, with a comparison of Inland (for example, Inland VA = the Chesapeake, its tributaries, Potomac tributaries, and seaside bays and inlets) vs. all ocean combined (state ocean + federal ocean).

weakfish stock assessment, such as changes in natural mortality, may need to be considered also when an operational model is considered.

This study provided not only useful spatially dynamic age-structured models but also a framework for fisheries scientists to explore possible ways to incorporate spatial dynamics into fisheries stock assessment models. Fish population dynamic patterns also may affect the performance of different models. Our study reflected characteristics of the example weakfish fishery dynamics across the North Atlantic under harvest, and hence the results are primarily applicable to the weakfish fishery. Results of our research are not intended to supersede results of the 2009 stock assessment for weakfish (NEFSC, 2009). Weakfish was used as a case study to demonstrate the applicability of these models to a wide range of species. Although the conclusion of an optimum model of spatial asynchrony may not be globally true for all southeastern US and Gulf of Mexico fisheries, the model-selection procedure, and the general conclusions on modelling Bayesian SCA with inconsistent or asynchronous relative abundance indices among surveys in different spatial area, have global utility.

Supplementary data

Supplementary material is available at the *ICESJMS* online version of the manuscript.

Acknowledgements

We thank Dr Hao Yu who helped produce the weakfish distribution plot (Figure 1). Special thanks to Jeff Brust from the Atlantic weakfish stock assessment subcommittee and Patrick Campfield from Atlantic States Marine Fisheries Commission who helped access the data. We also thank the Atlantic Weakfish Stock Assessment Subcommittee and ASMFC for providing comments and facilitating discussions on this manuscript. Specifically, we thank Jeff Brust, Victor Crecco, and Katie Drew for suggestions to improve the manuscript.

Funding

This research was supported by the USDA Cooperative State Research, Education and Extension Service, Hatch project #0210510 to Y.J., a grant for Model Complexity and Stock Assessment Quality awarded to Y.J. *et al.*, by the National Oceanic and Atmospheric Administration, and a grant for Improving Weakfish Stock Assessment awarded to Y. J. *et al.*, by the Virginia Marine Resources Commission.

References

Addis, P., Seccia, M., Manunzaa, A., Corriasa, A., Niffoia, A., and Caua, A. 2009. A geostatistical approach for the stock assessment of the edible sea urchin, *Paracentrotus lividus*, in four coastal zones of

Southern and West Sardinia (SW Italy, Mediterranean Sea). Fisheries Research, 100: 215–221.

Anselin, L. 2010. Thirty years of spatial econometrics. Papers in Regional Science, 89: 3–25.

ASMFC. 2006. 2006 Weakfish Stock Assessment: Weakfish Stock Assessment Report, Terms of Reference and Advisory Report, and Technical Committee Supplemental Material. Atlantic States Marine Fisheries Commission, Washington, DC. 315 pp.

Banerjee, S., Carlin, B. P., and Gelfand, A. E. 2003. Hierarchical Modeling and Analysis for Spatial Data. Chapman & Hall, Florida.

Berger, J. O. 1985. Statistical Decision Theory and Bayesian Analysis. Spring-Verlag, New York.

Bowman, A. W., and Azzalini, A. 1997. Applied Smoothing Techniques for Data Analysis. Oxford University Press, New York.

Buonaccorsi, J. P., Elkinton, J. S., Evans, S., and Liebhold, A. M. 2001. Measuring and testing for spatial synchrony. Ecology, 82: 1668–1679.

Burnham, K. P., and Anderson, D. 2002. Model Selection and Multimodel Inference. Springer-Verlag, New York.

Calder, C., Lavine, M., Muller, P., and Clark, J. S. 2003. Incorporating multiple sources of stochasticity into dynamic population models. Ecology, 84: 1395–1402.

Cheal, A. J., Delean, S., Sweatman, H., and Thompson, A. A. 2007. Spatial synchrony in coral reef fish populations and the influence of climate. Ecology, 88: 158–169.

Cowles, M. K., and Carlin, B. P. 1996. Markov Chain Monte Carlo convergence diagnostics: a comparative review. Journal of the American Statistical Association, 91: 883–904.

Cressie, N. 1993. Statistics for Spatial Data, Revised Edition. John Wiley and Sons, New York.

Draper, D. 1995. Assessment and propagation of model uncertainty (with discussion). Journal of the Royal Statistical Society, Series B., 57: 45–97.

Gelman, A. 2006. Prior distributions for variance parameters in hierarchical models (Comment on Article by Browne and Draper). Bayesian Analysis, 1: 515–534.

Gelman, A., Carlin, J. B., Stern, H. S., and Rubin, D. B. 2004. Bayesian Data Analysis. Chapman & Hall, London, UK. 668 pp.

Gelman, A., and Rubin, D. B. 1992. Inference from iterative simulation using multiple sequences (with discussion). Statistical Science, 7: 457–511.

Haynes, K. J., Liebhold, A. M., Fearer, T. M., Wang, G., Norman, G. W., and Johnson, D. M. 2009. Spatial synchrony propagates through a forest food web via consumer-resource interactions. Ecology, 11: 2974–2983.

Heino, M., Kaitala, V., Ranta, E., and Lindstrom, J. 1997. Synchronous dynamics and rates of extinction in spatially structured populations. Proceeding of the Royal Society of London, Series B, 264: 481–486.

Hudson, P. J., and Cattadori, I. M. 1999. The Moran effect: a cause of population synchrony. Trends in Ecology & Evolution, 14: 1–2.

Jiao, Y., Cortes, E., Andrews, K., and Guo, F. 2011. Poor-data and data-poor species stock assessment using a Bayesian hierarchical approach. Ecological Applications, 21: 2691–2708.

Jiao, Y., Hayes, C., and Cortés, E. 2009a. Hierarchical Bayesian approach for population dynamics modelling of fish complexes without species-specific data. ICES Journal of Marine Science, 66: 367–377.

Jiao, Y., Neves, R., and Jones, J. 2008. Models and model selection uncertainty in estimating growth rates of endangered freshwater mussel populations. Canadian Journal of Fisheries and Aquatic Sciences, 65: 2389–2398.

Jiao, Y., Reid, K., and Nudds, T. 2010. Consideration of uncertainty in the design and use of harvest control rules. Scientia Marina, 74: 371–384.

Jiao, Y., Reid, K., and Smith, E. 2009b. Model selection uncertainty and Bayesian model averaging in fisheries recruitment modeling. *In* The Future of Fisheries Science in North America, pp. 505–524. Ed. by R. J. Beamish, and B. J. Rothschild. Fish and Fisheries Book Series No. 31, Springer, New York.

Jiao, Y., Smith, E., O'Reilly, R., and Orth, D. 2012. Modeling nonstationary natural mortality in catch-at-age models: an example using the Atlantic weakfish (*Cynoscion regalis*) fishery. ICES Journal of Marine Science, 69: 105–118.

Lawson, A. B., Browne, W. J., and Vidal Rodeiro, C. L. 2003. Disease Mapping with WinBUGS and MLwiN. Wiley & Sons, West Sussex, England.

Legendre, P. 1993. Spatial autocorrelation: trouble or new paradigm? Ecology, 74: 1659–1673.

Liebhold, A., Koenig, W. D., and Bjornstad, O. N. 2004. Spatial synchrony in population dynamics. Annual Review of Ecology, Evolution and Systematics, 35: 467–490.

Lo, N. C., Jacobson, L. D., and Squire, J. L. 1992. Indices of relative abundance for fish spotter data based on delta-lognormal models. Canadian Journal of Fisheries and Aquatic Sciences, 49: 2515–2526.

MacCall, A. D. 1976. Density dependence of catchability coefficient in the California Pacific sardine, *Sardinops sagax caerulea*, purse seine fishery. CalCOFI Reports, 18: 136–148.

Massie, T. M., Weithoff, G., Kucklander, N., Gaedke, U., and Blasius, B. 2015. Enhanced Moran effect by spatial variation in environmental autocorrelation. Nature Communications, 6: 1–8.

Maunder, M. N., and Punt, A. E. 2004. Standardizing catch and effort data: a review of recent approaches. Fisheries Research, 70: 141–159.

Mohn, R. 1999. The retrospective problem in sequential population analysis: an investigation using cod fishery and simulated data. ICES Journal of Marine Science, 56: 473–488.

Moran, P. A. P. 1953. The statistical analysis of the Canadian lynx cycle. II. Synchronization and meteorology. Australian Journal of Zoology, 1: 291–298.

Nishida, T., and Chen, D. 2004. Incorporating spatial autocorrelation into the general linear model with an application to the yellowfin tuna (*Thunnus albacares*) longline CPUE data. Fisheries Research, 70: 265–274.

Northeast Data Poor Stocks Working Group (NDPSWG). 2009. The Northeast Data Poor Stocks Working Group Report, December 8–12, 2008 Meeting. Part B. Weakfish. US Dept Commer, Northeast. Fisheries Science Center Reference Document. 09-02. 373 pp.

Northeast Fisheries Science Center (NEFSC). 2008. Assessment of 19 Northeast Groundfish Stocks through 2007: Report of the 3rd Groundfish Assessment Review Meeting (GARM III), Northeast Fisheries Science Center, Woods Hole, Massachusetts, August 4–8, 2008. US Dept Commer, NOAA Fisheries, Northeast. Fisheries Science Center Reference Document. 08–15; 884 p + xvii.

Northeast Fisheries Science Center (NEFSC). 2009. 48th Northeast Regional Stock Assessment Workshop (48th SAW) Assessment Report. US Dept Commer, Northeast. Fisheries Science Center Reference Document. 09–15. 834 pp.

O'Brien, L., and Mayo, R. K. 1988. Sources of variation in catch per unit effort of yellowtail flounder, *Limanda ferruginea* (Storer), harvested off the coast of New England. Fishery Bulletin, 86: 91–108.

Pandit, A. N., Kolasa, J., and Cottenie, K. 2013. Population synchrony decreases with richness and increases with environmental fluctuations in an experimental metacommunity. Oecologia, 171: 237–247.

Pandit, S., and Kolasa, J. 2012. Opposite effects of environmental variability and species richness on temporal turnover of species in a complex habitat mosaic. Hydrobiologia, 685: 145–154.

Petitgas, P. 1993. Geostatistics for fish stock assessments: a review and an acoustic application. ICES Journal of Marine Science, 50: 285–298.

Petitgas, P. 2001. Geostatistics in fisheries survey design and stock assessment: models, variances and applications. Fish and Fisheries, 2: 231–249.

Pope, J. G., and Garrod, D. J. 1975. Sources of error in catch and effort quota regulations with particular reference to variations in the catchability coefficient. ICNAF Research Bulletin, 11: 1730.

Quinn, T., and Deriso, R. B. 1999. Quantitative fish dynamics. Oxford University Press, Oxford, UK.

Ricker, W. E. 1975. Computation and interpretation of biological statistics of fish populations. Available from Department of the Environment Fisheries and Marine Service, Ottawa, Canada. Bulletin of the Fisheries Research Board of Canada. No. 191.

Rose, G. A., and Leggett, W. C. 1991. Effects of biomass-range interactions on catchability of migratory demersal fish by mobile fisheries: an example of Atlantic cod (*Gadus morhua*). Canadian Journal of Fisheries and Aquatic Sciences, 48: 843–848.

Rossi, R., Mulla, D. J., Journel, A. G., and Franz, E. H. 1992. Geostatistical tools for modeling and interpreting ecological spatial dependence. Ecological Monographs, 62: 277–314.

Schabenberger, O., and Gotway, C. A. 2005. Spatial Methods for Spatial Data Analysis. Chapman & Hall, Florida.

Schnute, J. T. 1987. Data, uncertainty, model ambiguity, and model identification. Natural Resource Modeling, 2: 159–212.

Simard, Y., Legendre, P., Lavoie, G., and Marcotte, D. 1992. Mapping, estimating biomass, and optimizing sampling programs for spatially autocorrelated data: case study of the northern shrimp (*Pandalus borealis*). Canadian Journal of Fisheries and Aquatic Sciences, 49: 32–45.

Spiegelhalter, D. J., Best, N. G., Carlin, B. P., and van der Linde, A. 2002. Bayesian measures of model complexity and fit (with discussion). Journal of the Royal Statistical Society, Series B, 64: 583–640.

Spiegelhalter, D. J., Thomas, A., Best, N., and Lunn, D. 2004. WinBUGS User Manual (version 1.4.1). MRC Biostatistics Unit, Cambridge, UK.

Toni, T., and Stumpf, M. P. H. 2010. Simulation-based model selection for dynamical systems in systems and population biology. Systems Biology, 26: 104–110.

Vasseur, D. 2007. Environmental colour intensifies the Moran effect when population dynamics are spatially heterogeneous. Oikos, 116: 1726–1736.

Waller, L. A., and Gotway, C. A. 2004. Applied Spatial Statistics for Public Health Data. Wiley & Sons, New York.

Winter, A., Yu, H., O'Reilly, R., Orth, R., Berkson, J., and Jiao, Y. 2009. Weakfish CPUE Estimates Calculated with GLM and GAM Standardizations. ASMFC, Weakfish Stock Assessment Subcommittee. 62 pp.

Yu, H., Jiao, Y., and Winter, A. 2011. Catch rate standardization of yellow perch (*Perca flavescens*) in Lake Erie: a comparison between the Generalized Linear Model, Spatial Generalized Linear Model, and Generalized Additive Model. Transactions of the American Fisheries Society, 140: 905–918.

Handling editor: Ernesto Jardim